IDENTIFICATION OF ISOLATED CLUSTERED MICROCALCIFICATIONS BASED ON THE DISTRIBUTION OF EFFECTIVE ATOMIC NUMBER

V.A. Gorshkov[1] , N.I. Rozhkova[2], and S. P. Prokopenko[2]

[1]Space Research Institute

[2] Herzen Moscow Research Oncological Institute

Abstract

The goal of this work was to improve the efficiency of early detection of isolated clustered microcalcifications, the earliest indicators of breast cancer.

The presence of isolated clustered microcalcifications in the mammary gland significantly increases the range of variation of effective atomic number and significantly changes the form of its distribution. Isolated microcalcifications may not be visible at traditional mammograms. However, the fact of its presence in the mammary gland can be set analytically by the form of the distribution of the effective atomic number. The distribution of the effective atomic number in the tissue without microcalcifications is symmetrical and close to the normal law. But the breast with isolated clustered microcalcifications is characterized by asymmetry and high values of the maximum effective atomic number.The coordinates of the location of isolated microcalcifications can be calculated mathematically.

The histograms of maximum value of the reconstructed atomic numbers for 102 fragments of breast tissue without microcalcifications (301x301 pixels) (a) and for 48 fragments of breast tissue with microcalcifications were obtained. It is shown that the distributions of the reconstructed atomic numbers do not overlap. it proves that the type I errors (false positives , false conclusion about the presence of

microcalcifications) is practically equal to zero. However, the type II errors, (false negatives, skip microcalcifications) is related to its size granules, the number fragment pixel, the thickness of the breast and its assessment requires further research.

Introduction

Microcalcifications in the breast in 35% [1,2] of cases is an indicator of cancer. Detection of even a single microcalcification in the breast may indicate the beginning of the process of calcination, and of the origin of cancer disease. Despite considerable progress in the field of breast imaging [3] it is still difficult to detect a single microcalcification using traditional screening mammography, especially if its size is less than 100-150 μm. It is almost impossible to detect a single microcalcification by dual-energy subtraction [4] and dividing [5] mammograms, as well as by visualization of linear combinations of effective atomic number and density [6, 7]. The use of various filters in the visual processing of traditional mammograms [8] increases the contrast of the image, however, does not allow to identify isolated microcalcifications. The problem is not solved by using tomosynthesis [9]. Isolated microcalcifications are not detected and for scattered radiation [10].

Significant difference of the effective atomic number of microcalcifications from the atomic number of breast tissue may be the basis for their analytical identification.

Material and Methods

Traditional digital mammogram presents the visualization of the distribution of the proportion of photons that have passed the breast without interaction, which is defined for a source with a continuous spectrum as

$$\frac{N}{N_0} = \sum_{E=E_{min}}^{E=E_{max}} f(E) e^{-\mu_t(Z_t,E)\rho_t d_t - \mu_{mc}(Z_{mc},E)\rho_{mc}d_{mc}} \Delta E,$$

(1)

where N_0 - the initial number of photons,

N - the number of detected photons which have passed mammary gland without interaction, μ_i, ρ_i, d_i mass attenuation coefficients, density, thickness of the breast tissue (t) and microcalcifications (mc), respectively, $f(E)$ - a function of the density distribution of source energy defined by its spectrum, Z_t, Z_{mc} - effective atomic numbers of tissue and microcalcifications for $f(E)$, respectively, ΔE - value of the step in the discrete representation of the energy spectrum.

The presence of microcalcifications increases the effective atomic number of the breast area, because Z microcalcifications is 12-14, and the breast tissue - 6,3-7.

Despite the fact that the size of microcalcifications pellets (less than 0, 2 mm) is significantly less than the thickness, compressed breast on mammography (20-50 mm), their accumulation at mammograms appear very clearly. This is due to the fact that their density is more than twice the density of tissue, as well as the fact that the mass attenuation coefficient is proportional to the atomic number of the 3-4-th degree.

The ratio of mass attenuation coefficients for low and high-energy for monochromatic radiation determined by the ratio of the logarithms of the registered shares of radiation and depends only on the effective atomic number and is independent of the density

$$\beta(Z) = \frac{\mu_L}{\mu_H} = \frac{\ln \dfrac{N_0^L}{N^L}}{\ln \dfrac{N_0^H}{N^H}} \neq f(\rho). \tag{2}$$

The mass attenuation coefficients are determined by radiation energy and atomic number. But mammorgaphy is based on using sources with a continuous spectrum. In this case, the ratio of the logarithms will depend not only on the effective atomic number, but also on the density and thickness of the breast [11]

$$\beta(Z) = \frac{\ln \dfrac{N_0^L}{N^L}}{\ln \dfrac{N_0^H}{N^H}} = f(Z, \rho, d). \tag{3}$$

If for monoenergetic spectrum, the effective atomic number of the breast as a multicomponent object can be calculated, for the continuous spectrum, its value is not defined. And it is impossible to measure the mass attenuation coefficients of multicomponent structures for such spectrum.

The papers [11, 12] have shown that for continuous spectra mathematical mass attenuation coefficients must be used.

It is their ratio determines the effective atomic number which is invariant to the density and thickness of the breast.

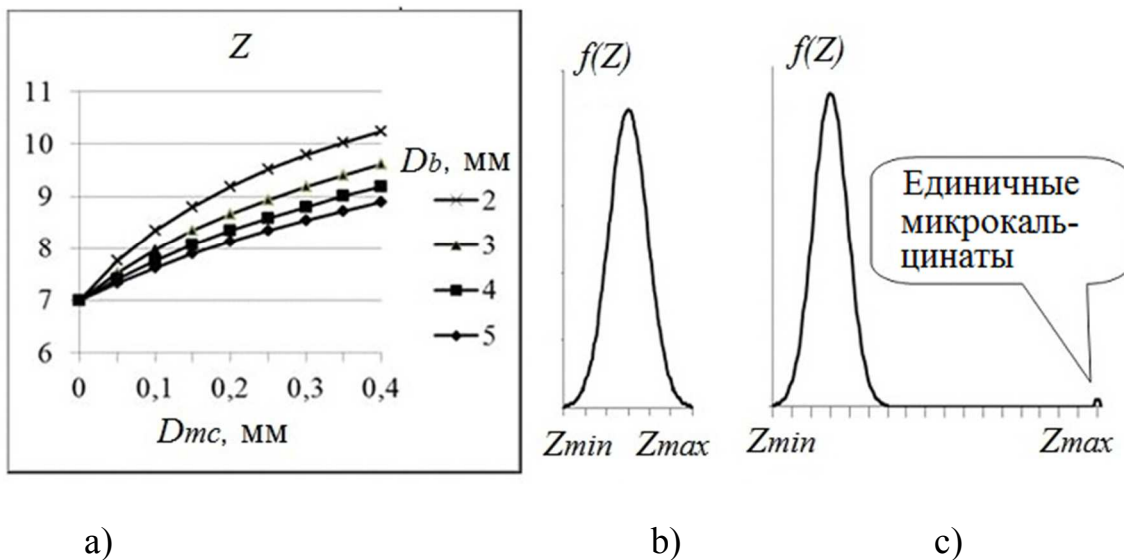a)   b)   c)

Fig. 1. The effect of the presence of microcalcifications on the distribution of the effective atomic number Z in the breast: a) - the dependence of the effective atomic number of breast tissue with microcalcifications on its size (D_{mc}) for varying its thickness (D_b); b) - the hypothetical distribution of Z in the breast without microcalcifications; c) - the same in the breast with microcalcifications

Figure 1 shows the dependence of the effective atomic number of breast tissue with microcalcifications on the its size for different breast thickness. The smaller the breast thickness, the higher the effective atomic number of the breast tissue with microcalcifications.

The distribution of effective atomic number in the mammary gland without microcalcifications is closed to the normal laws and is symmetrical in Zmin- Zmax range (Fig. 1b). However, the presence of at least one single microcalcifications leads to its asymmetry, since Z in this area is significantly higher. (Figure 1c).

The distribution of effective atomic number determines the fact of the existence of individual microcalcifications in the breast.

Results

The distributions of the reconstructed effective atomic number in the mammary glands without microcalcifications (Figure 2) is relatively constant and their values vary in a very wide range: 6 ... 10. Such variation is not determined by the distribution of the actual values of the effective atomic number in the breast, but low counting statistics of detected photons. The number of detected photons by the elemental detector of scintillator matrix is not more 100 photons. It leads to variation of the reconstructed effective atomic numbers in the mammary gland in the range of 12 ... 15%.
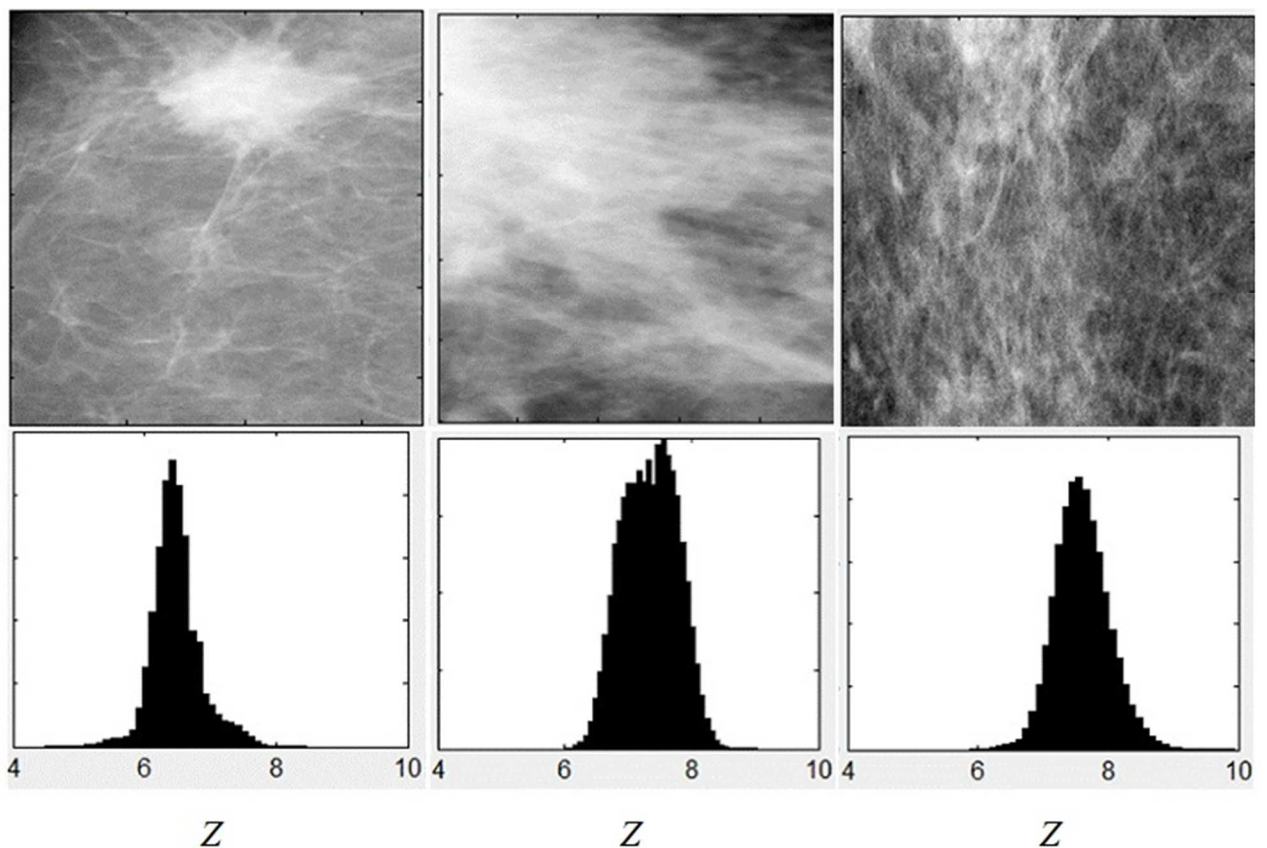

Figure 2. Three fragments of mammograms breasts (30x30 mm) without microcalcifications (top row) and the corresponding distribution of the reconstructed atomic numbers (bottom row)

Figure 2 shows three examples of distributions reconstructed effective atomic number in the breast without microcalcifications. As it is seen the maximum value does not exceed 10.

Figure 3 shows two examples of mammary gland with microcalcifications. The distribution of the reconstructed atomic number in the overwhelming number of pixels is similar to its distribution in the breast without microcalcifications. However, the presence of individual microcalcifications essentially shifts the distribution to the left. In this case the atomic numbers reach to inadequate significant values (18-20) that, of course, significantly exceed the value of the real effective atomic numbers (Figure 1).

a)   b)   c)
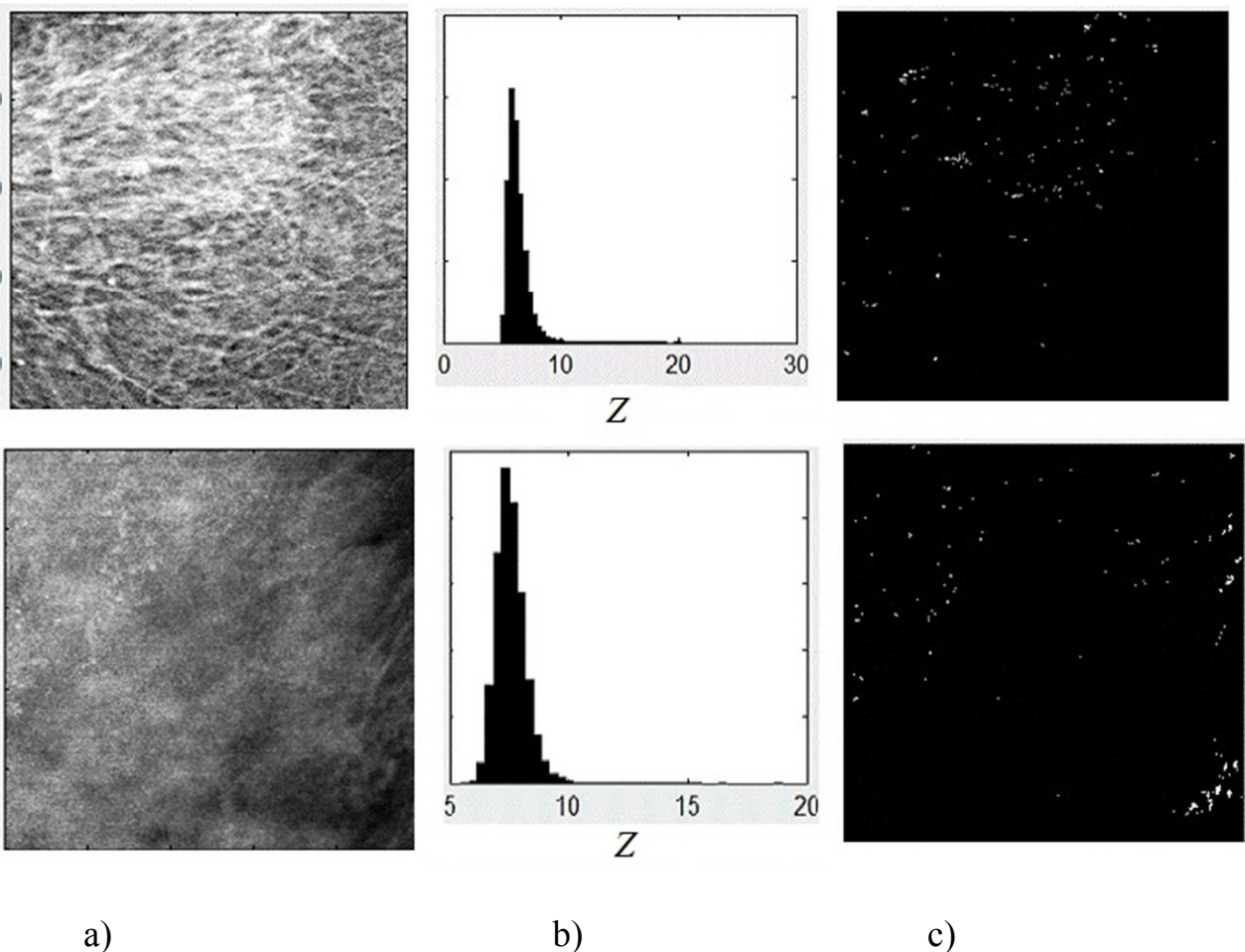
Figure 3. Two breast microcalcifications example, deposition in the milk ducts (top row) and breast cancer with severe diffuse fibrous mastopathy (bottom row): a) - fragments of mammograms; b) - the distribution of the reconstructed atomic number; c) - coordinates of the mammograms pixel, which correspond to microcalcifications locations

This overestimation is due to the impossibility to sync mammograms obtained at the high-energy and low-energy radiation perfectly.

This leads to the fact that the ratio of absorption coefficients of breast tissue with microcalcifications at low-energy μ_L^{t+mc} to absorption coefficients of breast tissue without microcalcifications at high-energy μ_H^t.

But this ratio is significantly greater than the ratio of the attenuation coefficients of tissue without microcalcifications and tissue with microcalcifications [4]

$$\frac{\mu_L^t}{\mu_H^t} < \frac{\mu_L^{t+mc}}{\mu_H^t} \quad \text{и} \quad \frac{\mu_L^{t+mc}}{\mu_H^{t+mc}} < \frac{\mu_L^{t+mc}}{\mu_H^t}.$$

(4)

This effect only heightens the sensitivity of the reconstructed atomic number to the presence of individual microcalcifications in the breast.

Figure 3c shows the calculated pixel coordinates of the mammogram where the reconstructed effective atomic number greater than 12.
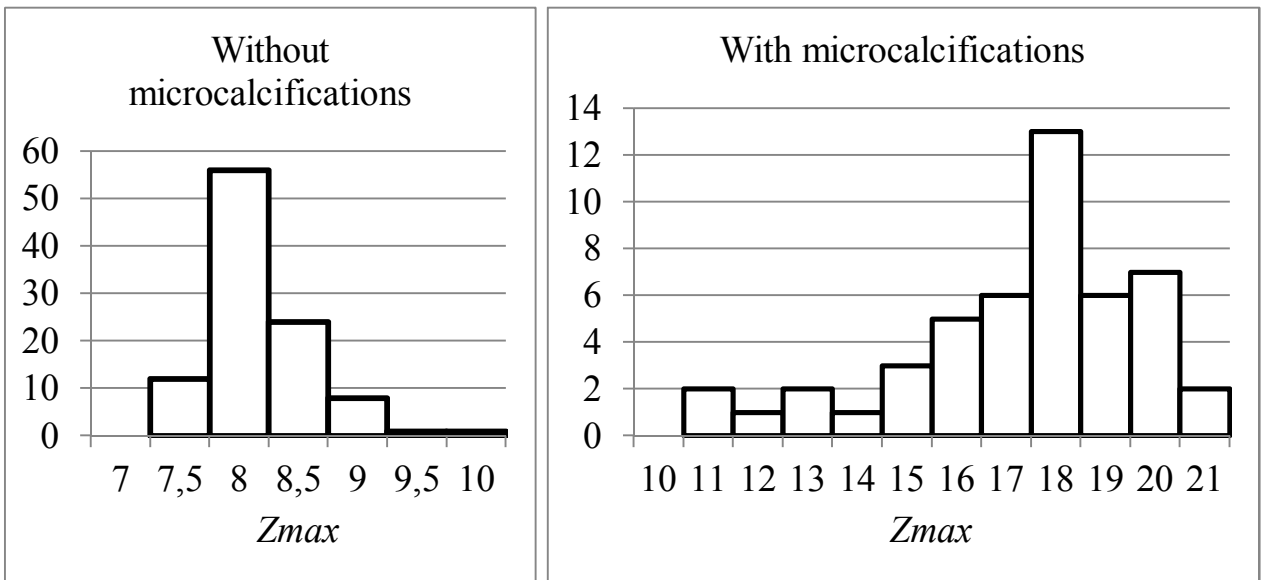
	Without microcalcifications	With microcalcifications
a)		b)

Figure 4. Histograms of maximum value of the reconstructed atomic numbers: a) for 102 fragments of breast tissue without microcalcifications; b) for 48 fragments of breast tissue with microcalcifications

Figure 4 shows the histograms of maximum value of the reconstructed atomic numbers for 102 fragments of breast tissue without microcalcifications (301x301 pixels) (a) and for 48 fragments of breast tissue with microcalcifications.

As it is seen, these distributions do not overlap. In this connection, we can assume that type I errors (false positives , false conclusion about the presence of microcalcifications) is practically equal to zero. However, type II errors, (false negatives, skip microcalcifications) is related to its size granules, the number fragment pixel, the thickness of the breast and its assessment requires further research.

Conclusion

The distribution of the reconstructed effective atomic number in the breast enables identification of isolated clustered microcalcifications which are not visible at traditional mammograms.

The fact of its presence in the mammary gland can be set analytically by the form of the distribution of the effective atomic number.

The coordinates of the location of isolated microcalcifications can be calculated mathematically.

Bibliography

1. *Murphy W.A, DeSchryver-Kecskemeti K.* Isolated clustered microcalcifications in the breast: radiologic-pathologic correlation // Radiology. 1978. Vol. 127(2). PP. 335-341.

2. Woo Kyung Moon, Jung-Gi Im, Young Hwan Koh, Dong-Young Noh, and In Ae Park.US of Mammographically Detected Clustered Microcalcifications. Radiology, Dec 2000, Vol. 217: 849–854. DOI: http://dx.doi.org/10.1148/radiology.217.3.r00nv27849

3. Bonnie N. Joe, Edward A. Sickles. The Evolution of Breast Imaging: Past to Present. // Radiology. November 2014Volume 273, Issue 2S. DOI: http://dx.doi.org/10.1148/radiol.14141233.

4. *Lewin J. M., Isaacs P. K., Vance V., Larke F. J.* Dual-Energy Contrast-enhanced Digital Subtraction Mammography: Feasibility // Radiology. 2003. Vol. 229(1); PP. 261-268.

5. *Gorshkov V. A., Rozhkova N. I., Prokopenko S. P.* Dual-Energy Diving Mammography // Digital Mammography 10th Inter. Workshop. IWDM 2010. Girona, Spain; PP. 606 – 613.

6. *V. A. Gorshkov, N. I. Rozhkov, and S. P. Prokopenko.* Ray Imaging of Microcalcifications Based on DualEnergy DividingSubtracting Mammography. Biomedical Engineering, Vol. 48, No. 5, January, 2015, pp. 277-281. DOI 10.1007/s10527-015-9470-5.

7. *V.A. Gorshkov, R.R. Nazirov, V,G, Rodin, N.I. Rozhkova , S.P.Prokopenko.* Verfahren zur Zwei-Energien-Divisions-Differenz-Mammographie // PCT WO/2013/136150. 2013.

8. *Alessandro Bria et al.* Deep Cascade Classifiers to Detect Clusters of Microcalcifications// Digital Mammography 13th Inter.Workshop. IWDM 2016; Malmo, Sweden; PP. 415 - 422.

9. *A. Mackenzie et al.* Effect of Dose on the Detection of Micro-Calcification Cluster for Planar and Tomosynthesis Imaging // Digital Mammography 13th Inter.Workshop. IWDM 2016; Malmo, Sweden; PP. 152 - 159.

10. *Rozhkova, V. A. Gorshkov, N. I. and S. P. Prokopenko.* Scattered X-ray radiation in diagnosis of mammary gland diseases. Biomedical Engineering. July 2006, Volume 40, Issue 4, pp 180–182.

11. *Gorshkov, Vjacheslav*. "The effective atomic number and the mass attenuation coefficient of a multicomponent object for the continuous spectrum of the radiation." Nondestructive Testing and Evaluation (2016): 1-11. DOI 10.1080/10589759.2016.1146718/

12. *N.I. Rozhkova, V.A. Gorshkov, E.V. Mesquite, et al*. Digital Breast Clinic. Modern imaging technology / Ed. N.I. Rozhkova, V.A. Gorshkov). - M .: Special Medical Publishing books, 2013. 160 pp. (in Russian).